iScience

CellPress
OPEN ACCESS

Article

A universal managing circuit with stabilized voltage for maintaining safe operation of self-powered electronics system

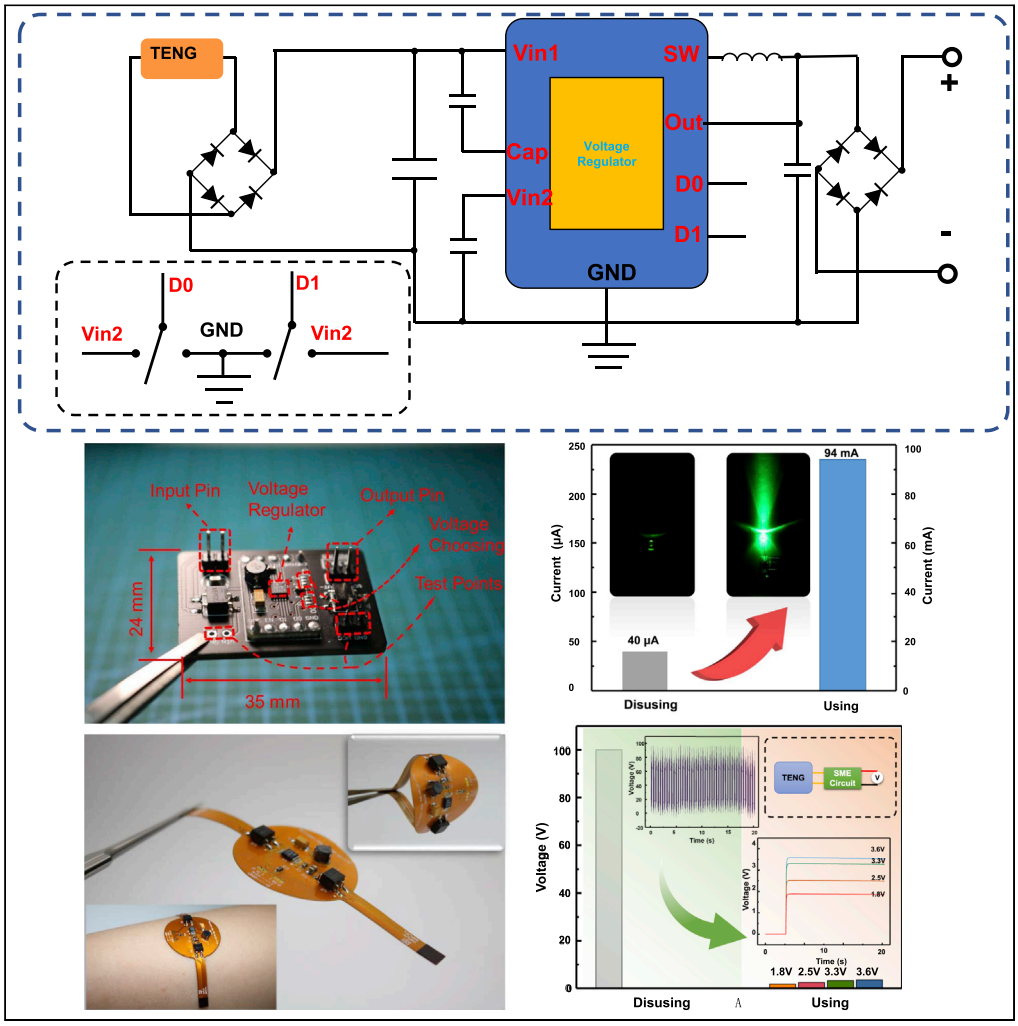

Fan Wang, Jingwen Tian, Yafei Ding, ..., Ya Yang, Xiangyu Chen, Zhong Lin Wang

yayang@binn.cas.cn (Y.Y.)
chengxiangyu@binn.cas.cn (X.C.)
zhong.wang@mse.gatech.edu (Z.L.W.)

Highlights

UMC is designed for a TENG to maintain stable voltage with a lower resistance

UMC provides a short-circuit current of 94 mA with an energy loss lower than 5%

UMC can completely avoid the breakdown of electronic devices due to TENG's high voltage

Three self-powered sensor systems have been successfully established

Wang et al., iScience 24, 102502
May 21, 2021
https://doi.org/10.1016/j.isci.2021.102502

iScience

CellPress
OPEN ACCESS

Article

A universal managing circuit with stabilized voltage for maintaining safe operation of self-powered electronics system

Fan Wang,[1,2] Jingwen Tian,[1,2] Yafei Ding,[1,2] Yuxiang Shi,[1,2] Xinglin Tao,[1,2] Xingling Wang,[1,2] Ya Yang,[1,2,*] Xiangyu Chen,[1,2,4,*] and Zhong Lin Wang[1,2,3,*]

SUMMARY

Harvesting mechanical energy via a triboelectric nanogenerator (TENG) is a promising strategy for solving energy problems. However, it is necessary to develop an effective and safe energy managing circuit for preventing high voltage breaking electronic devices. Here, a universal managing circuit is developed to optimize TENG's output performance, which for the first time allows the TENG to safely power various sensor systems with a safe and stable voltage. Based on the circuit, TENG's output can be transformed into a stable voltage with tunable amplitude, while an enhanced short-circuit current of 94 mA with an energy loss lower than 5% is achieved. For demonstrations, three different types of TENGs, respectively, targeting at ocean energy, wind energy, and walking energy have been prepared to reveal the capability of the circuit. This study offers a strategy to greatly enhance the output performance of TENGs to provide useful guidance for constructing self-powered and distributed sensor systems.

INTRODUCTION

Entering the era of internet of things, wearable and implantable electronic devices are in rapid development, leading to an urgent demand of clear, sustainable, and distributed energy supply (Tarancón, 2019; Say et al., 2020; Wang, 2018; Tang et al., 2020). Traditionally, batteries are employed to power these devices, while their limited capacity and big volume cannot fully satisfy the fast-rising demands (Liang et al., 2020a, 2020b, 2020c; Nyholm, 2020). Harvesting energy from ambient environment or human motion is one of most promising strategies to compensate the deficiencies of battery (Li et al., 2020a, 2020b; Zhang et al., 2018; Liu et al., 2020a, 2020b; García Núñez et al., 2019; Xue et al., 2017; Seol et al., 2015; Kim et al., 2018). First proposed by Wang Group in 2012 (Fan et al., 2012), the triboelectric nanogenerator (TENG, also called Wang generator), which can convert all kinds of mechanical energy into electricity, has so far been applied in many fields, including the exploitation of ocean wave energy (Liang et al., 2020a, 2020b, 2020c), harvesting human motions energy (Zhao and You, 2014; Ren et al., 2020a, 2020b; Miao et al., 2019), and even heartbeat energy (Ouyang et al., 2019; Liu et al., 2019a, 2019b). Driven by the Maxwell's displacement current, TENGs have significant high-voltage output, which can reach thousands of volts, while the current output of TENGs is very low within the microampere level, and the internal resistance is very large within the megohm level (Wang et al., 2020a, 2020b, 2020c; Liu et al., 2019a, 2019b; Xia et al., 2019; Zi et al., 2016a, 2016b; Li et al., 2020a, 2020b; Mao et al., 2017). Accordingly, an effective and safe energy managing system is quite necessary for TENG devices.

The working voltage and impedance of electronic device and energy storage unit are relatively low, which cannot match with the high voltage and internal resistance of TENGs, and thus, it is not possible to directly use TENGs as a power source for the electronic system (Harmon et al., 2020; Wang et al., 2020a, 2020b, 2020c; Xia et al., 2020; Wang et al., 2018). Meanwhile, mechanical energies in environment usually come from random mechanical motions, and the output signal from the TENGs has pulsed waveform with random amplitude and frequency. In order to regulate the output of TENGs, current boosting, buck converting, and energy storage are three important modules need to be considered (Cheng et al., 2019; Zhang et al., 2019). In the past few years, even though many significant improvements have been achieved in these directions, several unsolved issues are still hindering the practical applications of TENGs. First of all, the controlling circuits in most of managing circuits of TENGs are powered by another circuit, which requires external power

[1]CAS Center for Excellence in Nanoscience, Beijing Key Laboratory of Micro-nano Energy and Sensor, Beijing Institute of Nanoenergy and Nanosystems, Chinese Academy of Sciences, Beijing 100083, China

[2]School of Nanoscience and Technology, University of Chinese Academy of Sciences, Beijing 100049, China

[3]School of Material Science and Engineering, Georgia Institute of Technology, Atlanta, GA 30332-0245, USA

[4]Lead contact

*Correspondence: yayang@binn.cas.cn (Y.Y.), chengxiangyu@binn.cas.cn (X.C.), zhong.wang@mse.gatech.edu (Z.L.W.)

https://doi.org/10.1016/j.isci.2021.102502

supply or manual operation (Song et al., 2019; Cheng et al., 2017; Zhang et al., 2020). Therefore, a fully active power management (PMM) is quite necessary for TENGs. Secondly, traditional buck converting for managing output signal of TENGs including inductive transformer or passive switch cannot provide a stable output voltage signal, and it is difficult to be directly connected with electronic units (Zi et al., 2016a, 2016b; Zi et al., 2017; Xu et al., 2018; Pu et al., 2016). So far, a PMM specially designed for TENGs is still one of the most important tasks for the study of TENGs (Liu et al., 2020a, 2020b; Niu et al., 2015).

Here, we proposed for the first time a universal managing circuit (UMC) for TENGs, which is able to provide a stable and optional output voltage for matching standard electronic voltage, while its controllable output current can be up to 94 mA. This managing circuit with stable output voltage can directly supply power to the sensor system, avoiding the breakdown of electronic devices due to TENG's high voltage, and can connect directly with high-voltage TENGs and well match the high output impedance of TENGs with no additional power supply. Both the voltage and the current can also be regulated by the inner capacitor of the managing circuit which allows charge to be accumulated on an input capacitor until the buck converter can efficiently transfer a portion of the stored charge to the output. Meanwhile, the charging speed of a TENG-capacitor system is increased 2.5 times with the help of this managing circuit. Three demonstrations with different types of TENGs have been prepared to reveal the capability of this managing circuit, and the output signal from this managing circuit can be directly used to power various low power devices, such as an ocean temperature monitor, humidity sensor, Bluetooth transmitter for position detecting, and so on.

RESULTS AND DISCUSSION

A framework for a self-powered sensor system based on TENGs is illustrated in Figure 1A. A fully self-powered wireless environment sensor system requires microcontrollers and transducers that collect energy from environments. The link between an energy generator and energy consumer is the energy managing circuit. The typical working principle of a TENG is shown in Figure 1B, where a contact-separation TENG is selected as the example, and the universal managing circuit is aiming at serving all kinds of TENGs. Usually, nanostructures are designed on the surface of triboelectric materials to further enhance the output performance of the TENG. For example, the poly tetra fluoroethylene (PTFE) film with nano-patterns on its surface (water contact angle of 156°) is modified by the inductively coupled plasma etching treatment, as shown in Figure 1C including **i** and **ii**. As shown in Figure S1, the nano-structured PTFE improved the TENG's output performance. The detailed fabrication process is presented in STAR Methods section. The performance of TENGs can be enhanced and regulated by the managing circuit, while the stable voltage the direct current (DC) outputs provided by the managing circuit can power various functional devices with a standard electronic voltage, such as sensors, alarming devices, displaying devices, and so on. As shown in Figure 1D, the universal managing circuit can transfer the AC output of TENGs into a stable DC output with high current value and stable voltage value. For improving the wearable performance, a flexible and soft circuit is also designed to meet different application scenarios as shown in Figure 1E. The detailed fabrication process of managing circuit is presented in the Transparent Methods supplemental information. Figures 1F–1H show the superior output performance of TENGs under the management of the managing circuit. With the managing circuit, the high voltage pulses of TENG can be gathered, while the collected charges can be released at once. Then, a current pulse signal with the amplitude of dozens of milliampere can be produced. Moreover, the voltage stabilizing module in the managing circuit can regulate the voltage of the output signal to be a stable value, not in the form of pulses, as shown in Figure 1F. The voltage value can be designed to be 1.8V, 2.5V, 3.3V, or 3.6V, which are the common operation voltage of various electronics devices. The TENG with the managing circuit can offer a current output in the milliampere scale, lighting up a very bright light-emitting diode (LED) (see Figure 1G **ii** and Video S1), while the same TENG without universal managing circuit can only provide current output in the microampere scale (see Figure 1G i). With high current and stable voltage, the UMC-based TENG with milliampere level current can light UV LED very bright, which can be used as a self-powered currency detector (see Figure S2 and Video S2). Moreover, the amount of single charge transfer of the TENG with universal managing circuit is about 2.88 times of that the TENG just with a simple AC-DC rectifier bridge, as shown in Figure 1H.

The managing circuit is diagrammed in Figure 2A, mainly consisting of two full bridge rectifiers, a voltage regulator, and some capacitors. As explained in above part, the circuit has two major functions. The first one is to collect and store the output charges from the TENG, in order to realize a high current output. The second is related to the voltage stabilizing function, which can release the stored charge at the designed voltage value.

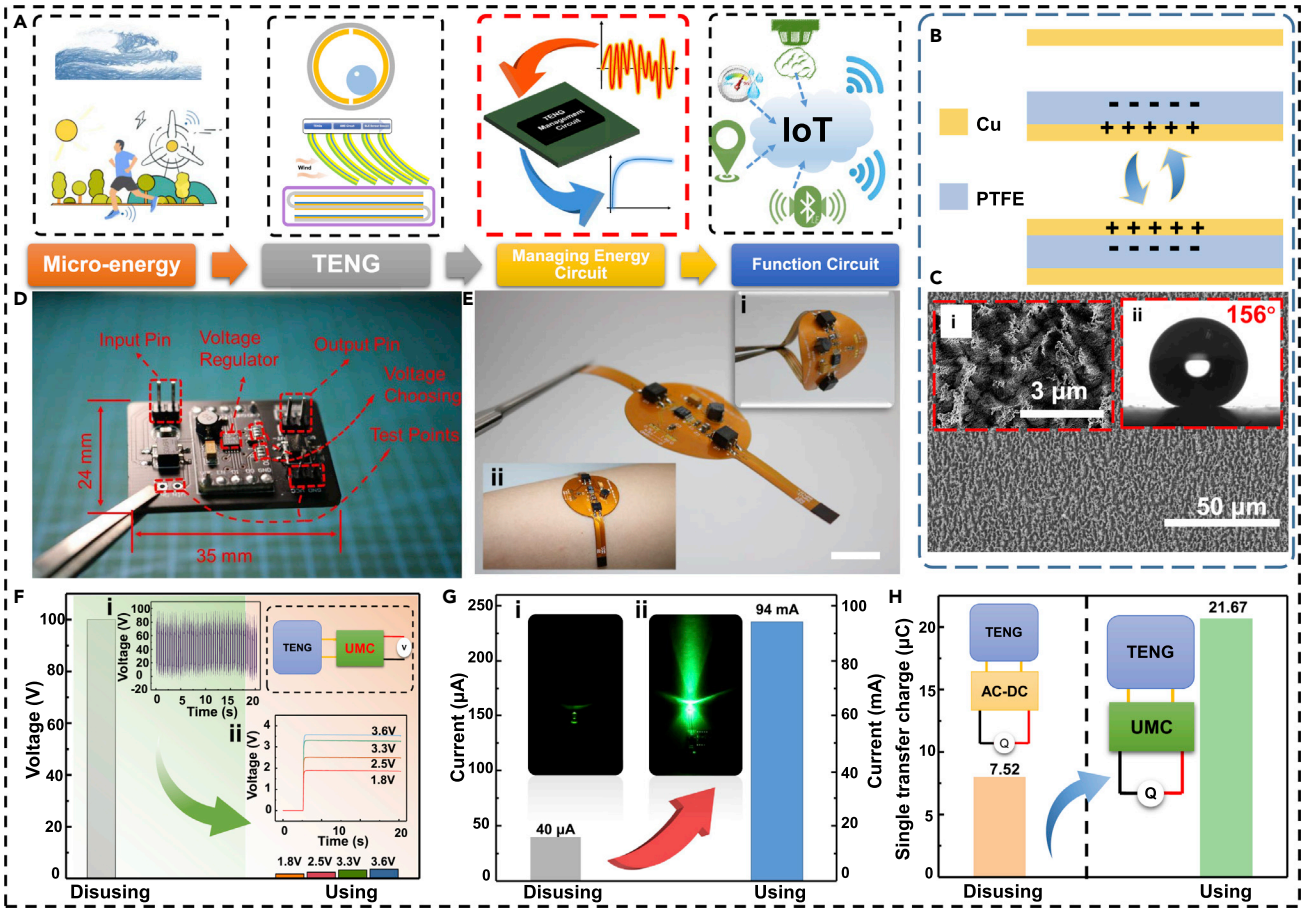

Figure 1. Structure design of the self-powered system based on the universal managing circuit and TENG

(A) Framework for the self-powered sensor system achieved by a universal managing circuit with TENGs harvesting micro-energy.

(B) Working principle of each TENG unit.

(C) Scanning electron microscope (SEM) images of the PTFE polymer nanostructure (including i) and (ii) its surface with water contact angle of 156°.

(D) Photograph of a hard universal managing circuit with its size and pins.

(E) Photograph of flexible and soft universal managing circuits (the scale bar is 1 cm). (i and ii) Photographs show its softness and flexibility.

The superior output performance of the TENG under the universal managing circuit in (F) output voltage, (G) current, and (H) single charge transfer, respectively.

The high efficiency voltage regulator and one buck converter are contained in the chip LTC 3588-1 (see Figure S3). It should be emphasized that the commercial chip LTC 3588 cannot directly connect with high-voltage TENGs because the chip's input voltage cannot stand with the voltage signal larger than 20 V. Hence, it is necessary to establish an external circuit to manage the high voltage signal of the TENG and only use the reaction loop of the chip LTC-3588. This management circuit is specially designed for the TENG, which is totally different from traditional application of the chip LTC-3588. The first rectifier D1 can transform the alternating current output of the TENG into direct current. The second one is to further rectify the output current to ensure that the function circuit is working properly. The charges are stored in the input capacitor C1 and then transferred by the voltage regular to the output capacitor C4. The target output voltage can be set to 1.8V, 2.5V, 3.3V, or 3.6V, by connecting pin D0 and D1 to pin of input voltage 2 (Vin2) or ground (GND) (see Table S1). Therefore, the pin D0 and D1 are connected to Vin2 and GND, respectively, to match the working voltage of the electronic device in the next experiments.

LTspice software is used to simulate the universal managing circuit; related parameters are shown in Table 1. The simulation result with respect to various external Cap (C1) is plotted as Figure 2B. The output current increases with the increase of external Cap (C1). As shown in Figure 2C, when the voltage of C1 charging by TENGs increase to 5.2V, the voltage regulator controls the C1 to discharge then the voltage of C1

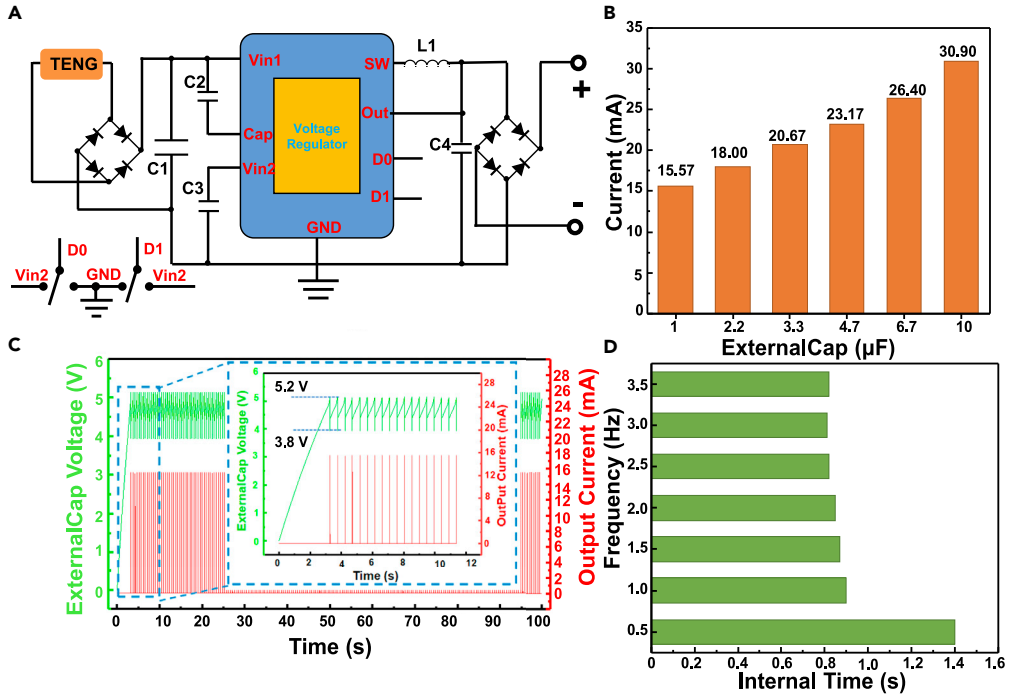

Figure 2. Circuit structure and stimulation of the universal managing circuit

(A) Circuit diagram of the universal managing circuit.

(B) Stimulation result of output current with different external Cap (C1).

(C) The voltage of external Cap (C1) charging by TENG and the output current of the universal managing circuit.

(D) Simulation result of internal time between two current peaks with respect to various low frequencies.

decreases to 3.8V, meanwhile the output current is significantly increased, with a peak value above 15.57 mA. Moreover, with the increase of frequency of input signal, the interval time between current peaks becomes smaller (see in Figure 2D).

To explore the performance of this universal managing circuit, the grating-structured freestanding TENG (GF-TENG) is applied to work with the managing circuit, and a basic operating unit is sketched in Figure 3A. It has a PTFE film with a metal electrode deposited on the back side (back electrode). On the front side, the PTFE film makes relative motion with another metal electrode (contact electrode). During contact, electrons are transferred from metal into PTFE, leading to the accumulation of negative charges on PTFE surface and positive ones on metal surface. COMSOL Multiphysics software based on finite-element simulation is employed to calculate the potential distribution across the two electrodes at different states, as shown in Figure 3B, and the variation of this potential difference induces displacement current in the external circuit. Figures 3C–3E show the output performance of the GF-TENG at 2Hz without universal managing circuit. The open-circuit voltage can reach to 100 V, and the short-circuit current is about 40 μA. With the AC-DC rectifier bridge, the amount of single charge transfer is about 7.52 μC. The stable value of the output voltage as well as the output current is shown in the table of Figures 3F and 3G, and a video demonstration with LED light is shown in Supporting Videos S1 and S2. The output current of the TENG integrated with the universal managing circuit is significantly increased, with a peak value above 14.3 mA under C1 of 3.3 μF. The amount of transferred charges corresponding to one current peak is over 21.67 μC, as shown in Figure 3H. The charge transfer efficiency (η) of the universal managing circuit can be calculated based on the following equation:

$$\eta = \frac{Q_{out}}{nQ_{TENG}}$$

here, Q_{out} from managing circuit is about 21.67 μC, n = 3 is charging cycles of the TENG, and Q_{TENG} is 7.52 μC. Hence, the efficiency η of the universal managing circuit is calculated to be about 96.1%, which means the energy loss within this managing circuit is lower than 5%. As shown in Figure 3I, when the voltage of external Cap (C1) is charging by TENG increase to about 5.2 V, the voltage regulator controls the C1 to

Table 1. Parameters used for simulating the universal managing circuit

Electronic device	Quantity	Unit
C2	1	μF
C3	4.7	μF
C4	10	μF
L1	10	μH

discharge; then, the voltage of C1 decreases to 3.8V, meanwhile the output current is significantly increased to a peak value, which is basically similar to the previous circuit simulation. The amplitude of the external Cap (C1) charging curve variation is basically maintained in the range of 3.8V–5.2V, as shown in Figure S4. For exploring the influence of the external Cap (C1) on the output current, the output short-circuit current is measured under different capacitors. When the external Cap (C1) is 47 μF, the short-circuit current is about 94 mA (see Figure 3J). As shown in Figure S5, the interval time of output current decreases with the increase of force, but the peak value remains basically unchanged. Finally, we use the same TENG with and without managing circuit to charge a capacitor of 470 μF. It has been found that the charging speed of the TENG with a managing circuit is 2.5 times faster than that without a managing circuit, as shown in Figure 3K. When the capacitor voltage reaches 3.3 V, the voltage will maintain stable at 3.3 V, which can protect the subsequent electronic devices or sensors from high voltage breakdown. As shown in Figures S6A and S6B, the best matching resistance of UMC-based GF-TENG (500Ω) is much smaller than the best matching resistance of GF-TENG (1MΩ), which is helpful for UMC to be used in practical functional circuits. Moreover, the maximum power of UMC-based GF-TENG is three times of the maximum power of GF-TENG, as shown in Figure S7.

The managing circuit can be applied for facilitating the energy harvesting of ocean waves. As can be seen in Figure 4A, a wireless ocean sensory system based on rolling-structured TENG (RS-TENG) and universal managing circuit is prepared. The schematic diagram of two polymethyl methacrylate spherical shells as well as the related TENG device is shown is Figures 4B and 4C. The inner shell is an RS-TENG consisting of a rolling PTFE ball and two stationary Cu electrodes as the electrification materials as shown in Figure 4B (i) and (ii). Driven by wave vibrations, the freestanding ball can roll back and forth between the two electrodes, providing alternating current to the external load. The outer shell can isolate electronic devices from seawater and keep stable environmental humidity for the operation of generators. The universal managing circuit and a Bluetooth low energy (BLE) sensor beacon are placed in the gap between the two polymethyl methacrylate spherical shells, where poly lactic acid made by 3D printing can help to fix the position shift. The BLE sensor beacon and its receiver are shown in Figure S8. In detail, diameters of the outside shell sphere and inside one are 9 cm and 7 cm, respectively, and the diameter of the PTFE ball is 2 cm, as shown in Figure 4C i, ii, and iii. The operating principle of the proposed RS-TENG is based on the conjugation of the triboelectric effect and electrostatic induction. When the freestanding PTFE ball rolls on the top of the right-hand Cu electrode, equal amounts of charges with different polarities generate on the top surface of the Cu and the surface of the PTFE ball (Figure 4B (i)). When the PTFE ball rolls from the right electrode toward the left electrode, the negative charges flow from the left electrode to the right electrode via the external circuit due to the electrostatic induction (Figure 4B (ii)). COMSOL Multiphysics software based on finite-element simulation is employed to calculate the potential distribution across the two electrodes at five different states, as shown in Figure 4D i-v, and the variation of this potential difference induces displacement current in the external circuit.

A simplified condition with continuous water ware is prepared, while three wireless ocean sensors are tested with real water ware, as shown in Figure 4E and Video S3 of the supplemental information. The temperature of the water and the humidity of the inside ball can be recorded by these wireless ocean sensors, and the related data can be sent to the receiver on the computer side via wireless BLE sensor beacon (see computer screen). The whole process of data recording and data sending is powered by the shell TENG with universal matching circuit. In detail, as shown in Figure 4F, the universal managing circuit integrated in a spherical TENG can power a BLE sensor beacon to monitor the temperature and humidity change. The energy from the TENG with UMC can support the BLE sensor beacon to send the hexadecimal data to the receiver on the computer, while the stable output voltage of UMC-based TENGs can match the voltage of the BLE sensor beacon. Finally, the computer translates hexadecimal data from all three BLE sensors into decimal data information and shows all these data in the form of tables and color cloud diagrams. The

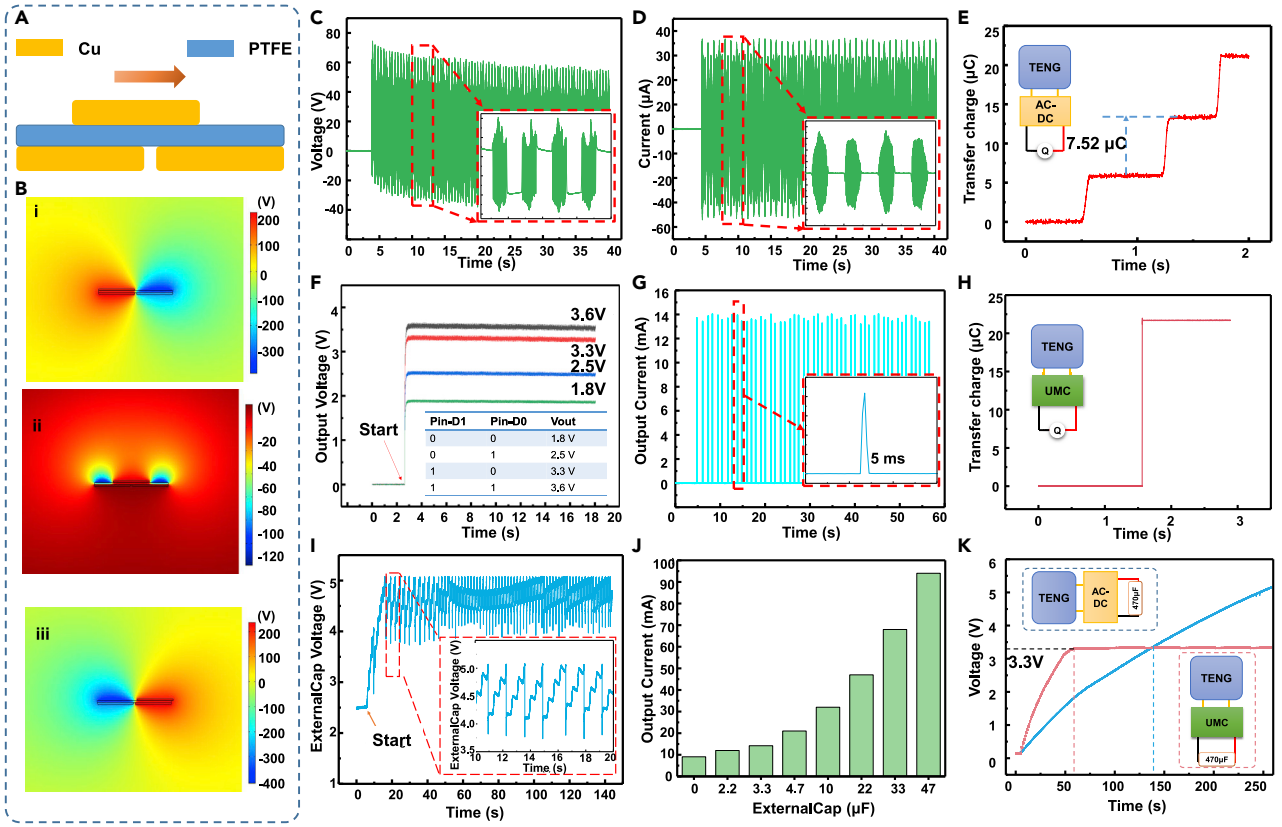

Figure 3. Comparison of the results of electric measurements for a GF-TENG and UMC-based TENG

(A) Schematic working principle and material composition of GF-TENG.

(B) The simulated potential distributions for the TENG at three different rolling displacements by COMSOL software employing the finite element method (FEM).

Measurement results of the (C) open-circuit voltage, (D)short-circuit current, and (E) amount of transferred charges of the GF-TENG (E), respectively. Inset of (E): connection with rectifier bridge AC-DC for the measurement of amount of transferred charges.

Measurement results of the (F) open-circuit voltage, (G) short-circuit current, and (H) amount of transferred charges of the UMC-based TENG, respectively. Inset of (H): connection with rectifier bridge AC-DC for the measurement of amount of transferred charges.

(I) The voltage of external Cap (C1) charging by UMC-based TENG and the output current of UMC-based TENG.

(J) Measured output current with variable external Cap (C1).

(K) Comparison for the charging performance of the UMC-based GF-TENG and GF-TENG.

details of the charging processes and waveform of BLE sensor are shown in Figure S9. In order to further verify the contribution of the universal managing circuit to the operation of ocean wave TENGs, we connected the output terminal of the universal managing circuit to a capacitor (400 μF). The capacitor can be charged to 3.26 V within 4 min with the help of the universal managing circuit. Meanwhile, if we remove the universal managing circuit, the same TENG needs about 8.5 min to charge the similar capacitor, as shown in Figure 4G. The output current of RS-TENG and UMC-based RS-TENG is shown in Figures S10 and S11, respectively. The long-term stability of the device is a very important parameter for the real operation of these self-powered systems. As shown in Figure 4H, the wireless distribution ocean sensor system is put in the actual water wave environment for 7 hr, and the three BLE sensor beacons can stably send their data to the computer receiver. As shown in Figure S12, the time required to collect the charges by UMC is about 1.5 min. Hence, the TENG combined with universal managing circuit can offer a feasible power solution to the long-term, wide-area, and near real-time monitoring of climate change in the open sea.

The similar environmental sensor system can also be driven by flexible leaf-shaped TENGs (LS-TENGs) and natural wind energy. As shown in Figure 5A, LS-TENGs collect wind energy, and the universal managing circuit converts the energy into suitable electrical signals that can directly drive environmental sensors. Then, environmental information data can be transmitted to the mobile phone through low-power Bluetooth, as shown

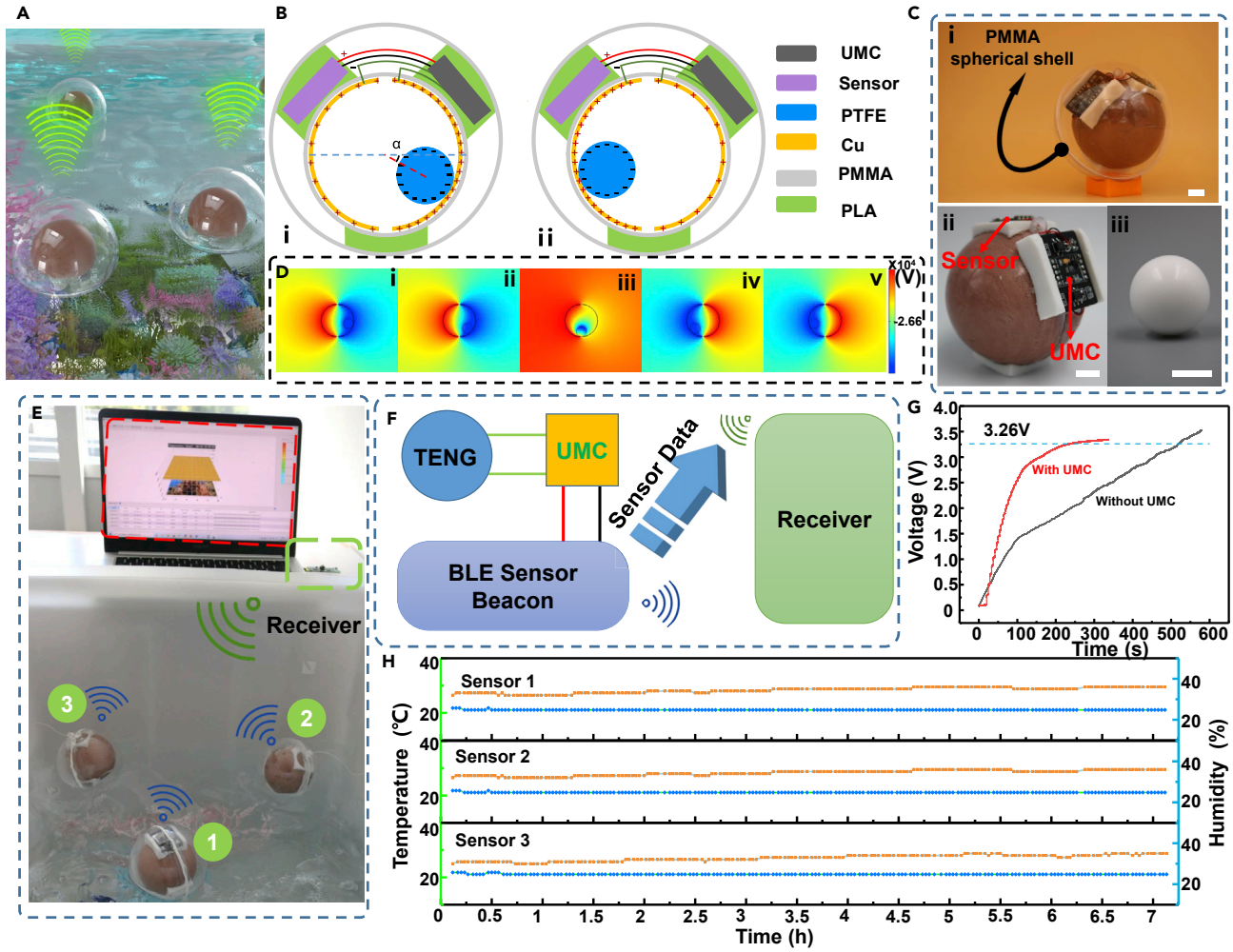

Figure 4. A demonstration of a wireless distribution ocean sensor system based on RS-TENG and UMC

(A) Photograph of wireless distribution ocean sensor balls floating on seawater.

(B) Structure and basic operations of an ocean senor system ball integrated with RS-TENG and UMC.

(C) (i) Photograph of one integral ocean senor system ball as fabricated. (ii) Photograph of an RS-TENG, sensor, and UMC, and (iii) photograph of one PTFE ball (the three scale bars represent 1 cm.).

(D) The simulated potential distributions for an RS-TENG at five different rolling displacements by COMSOL software employing the finite element method (FEM).

(E) Photograph showing three integral ocean senor system balls sending data to the receiver.

(F) System diagram of a wireless distribution ocean sensor system based on RS-TENG and UMC.

(G) Charging curves comparison of 400 μF under RS-TENG with UMC and without UMC.

(H) Temperature and humidity data from three wireless distribution ocean sensor balls working for 7 hr.

in Video S4 and Figure S13. An environmental sensor system based on flexible LS-TENGs is exhibited in Figure 5B, which is consisted of three parts: TENGs, universal managing circuit, and BLE sensor beacon. The TENG is a typical leaf-shaped device with six strips made by a PTFE film, Cu foil, and polyethylene terephthalate (PET) film, while the detailed design concept can be found in the previous studies (Ren et al., 2020a, 2020b; Zheng et al., 2018; Wang et al., 2020a, 2020b, 2020c; Xu et al., 2020). The contact-separation motions of six strips orderly can harvest environmental wind energy (Ren et al., 2019; Zhang et al., 2016). PET is selected as the backbone of the strip, mainly owning to its decent strength, low cost, and good machinability. In order to enhance the effective contact area of PTFE polymer and Cu, the nanostructure of PTFE polymer surface is created on the exposed PTFE surface by a top-down method of reactive ion etching. In order to consolidate the working principle of the TENG, COMSOL is employed to simulate the periodic potential variation between the two electrodes during contact-separation motions, as demonstrated in Figure 5C i and ii.

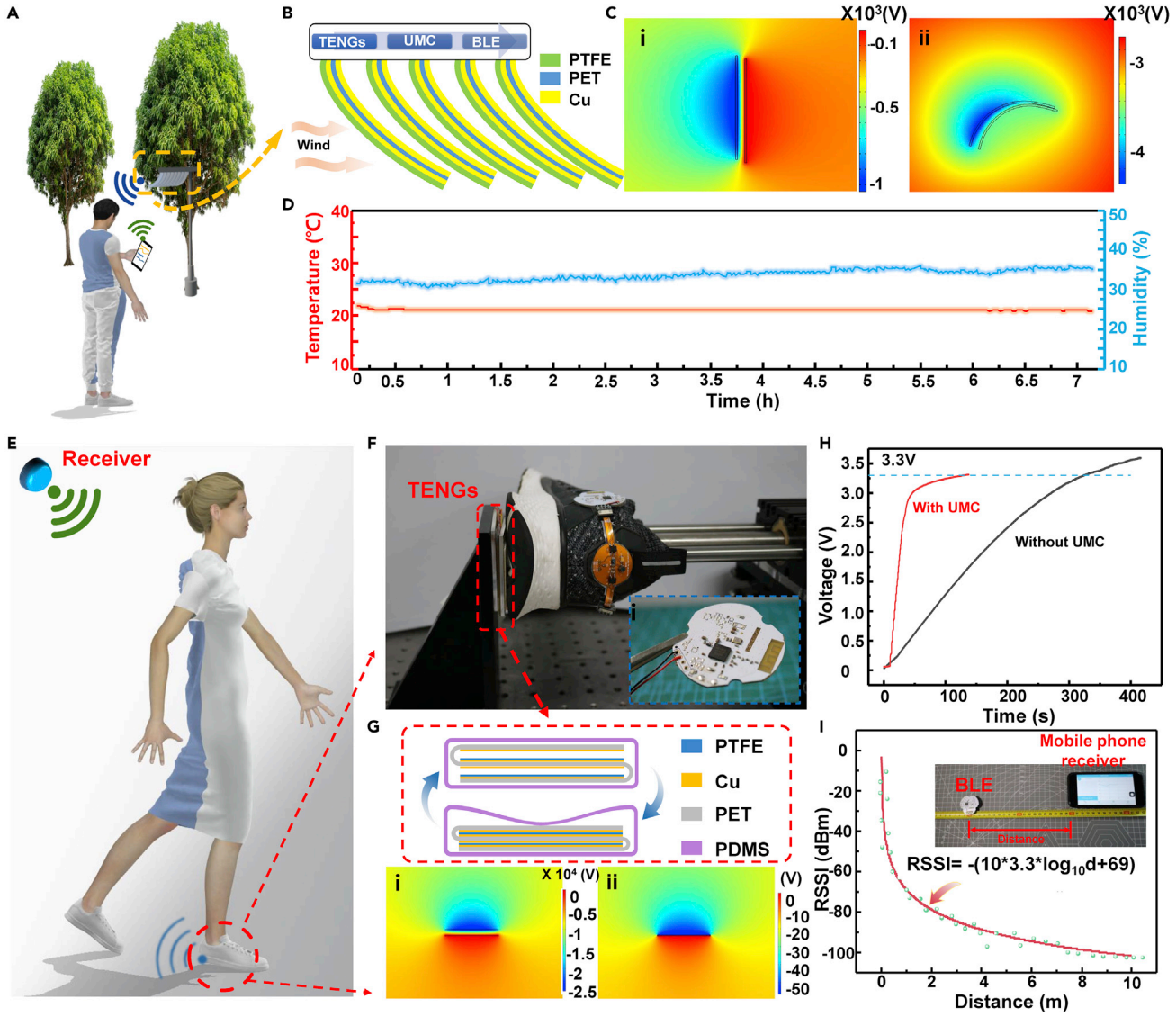

Figure 5. Two demonstrations of a wireless environmental sensor system and a self-powered indoor position system

(A) Photograph of a wireless environmental sensor system harvesting wind energy and sending environmental sensor data to the mobile phone.

(B) Structure and basic operations of a wireless environmental sensor system integrated with LS-TENGs and the universal managing circuit.

(C) The simulated potential distributions for an LS-TENGs unit by COMSOL software employing the finite element method (FEM).

(D) Temperature and humidity data from a wireless environmental sensor system working for 7 hr.

(E) The TENG and BLE Bluetooth assembled into the shoes to serve as a self-powered indoor position system.

(F) Simulation of a realistic human walking by using a linear motor for drive the layer TENG. Inset (i) is the photography of BLE beacon.

(G) Illustration of the working mechanisms of the TENG, and potential distribution for the distance between two triboelectric layers (or air gap) changes from 2 to 0.1 mm.

(H) Charging curves comparison of 470 μF under the layer TENG with UMC and without UMC.

(I) The variation of RSSI with different distances.

The long-term stability of the device is shown in Figure 5D, where the wireless environmental sensor system is put in the actual windy environment for more than 7 hr and the BLE sensor beacon can stably send environmental information data to the computer receiver.

In addition to this environmental energy harvesting, the universal managing circuit can also work with the TENG for collecting energy from human daily motions. For example, as shown in Figure 5E, the multilayer TENG integrated with human shoes can harvest energy from walking, while the universal managing circuit

helps to achieve a sustainable power supply for mobile BLE beacon. The stable output voltage of UMC-based TENGs can match the voltage of the BLE beacon. Accordingly, the self-powered indoor position system based on this multilayer TENG is illustrated in Figure S14. During the measurement, the multilayer TENG is driven by linear motor with a motion frequency of 1 Hz, as shown in Figures 5F and Video S5, while the universal managing circuit is made by soft substrate, in order to work with this wearable system. The detailed fabrication of the soft universal managing circuit is shown in Experiment part and Figure S15. As shown in Figure 5G, the electrification layers (PTFE and Cu) of the multilayer TENG show continuous contact-separate motions during human walking. This contact-separation working mechanism ensures little abrasion of the two surfaces, which helps to enhance the durability of the TENG. The basic working principle of this contact-separation mode of TENGs is simulated by using COMSOL software (see Figure 5G i and ii), which utilizes the conjugation between contact electrification and electrostatic induction. The capacitor of 470 μF should be charged to 3.3 V, in order to power the BLE beacon for transmitting the signal to receivers. It has been found that the charging speed of this multilayer TENG with universal managing circuit is increased about 2.4 times, as shown in Figure 5H. The peak of output current of the multilayer TENG is about 7.2 μA, while this value can reach 15.3 mA with the help of the universal managing circuit, as shown in Figures S16 and S17 .

The value of received signal strength indicator (RSSI) represents the distance from the receiver to the transmitter (BLE beacon). To estimate the distance based on the signal from a BLE beacon, a path loss model is needed. Here, we adopt the path loss model (Zuo et al., 2018):

$$RSSI = -(10n log_{10}d + A)$$

where parameter A is the absolute RSSI value represented by dBm at 1 m away from the beacon, n is a parameter related to the signal propagation environment, and d is the distance from the beacon. In our implementation, we use this method to estimate the parameters. The RSSI of BLE beacon is measured under different distances between Bluetooth and receiver (mobile phone) as shown in Figure 5I. Finally, the path loss model with pre-defined parameter in our implementation is $RSSI = -(10 * 3.3 * log_{10}d + 69)$

In order to determine the specific coordinates of a point in a two-dimensional plane, three receivers are used to get three distances from the point. The detail of how to position the person wearing the position system is shown in Figure S18A and S18B (supplemental information). This demonstration not only offers a strategy to power the BLE beacon by TENGs but also provides useful guidance for constructing a self-powered position platform used in special environment like mine and underground parking.

Conclusions

In summary, we have developed a different universal managing circuit as a link between TENG and functional electronics devices, such as wireless environmental sensors or microcontrollers. The universal managing circuit integrated with the TENG, well matching the high output impedance of TENGs, can provide an output current in the milliampere level, while the stable output voltage from this universal managing circuit can be stabilized at a designed value to power different wireless devices for preventing high voltage breakdown. The energy managing process of this circuit can be achieved automatically without the need of extra battery source, and the energy loss within this managing circuit can be maintained to be lower than 5%. The universality and efficiency of this universal managing circuit is verified by using the TENG with different working modes and structures. Three environmental sensor systems, which can harvest different micro-energies (water wave energy, windy energy, and walking energy), are demonstrated to verify the stability, versatility, and practicality of the universal managing circuit. The proposed universal managing circuit can be used for constructing wireless and distributed sensor systems with minimized energy consumption to meet challenges arose from robotics, wearable devices, environmental monitors, and the era of internet of things.

STAR★METHODS

Detailed methods are provided in the online version of this paper and include the following:

- RESOURCE AVAILABILITY
  - Lead contact
  - Materials availability
  - Data and code availability

- METHOD DETAILS
  - Fabrication of the hard and soft universal managing circuit
  - Fabrication of the polymer nanostructures on the surface of the PTFE thin film and materials characterization
  - Electric measurements device

SUPPLEMENTAL INFORMATION

Supplemental information can be found online at https://doi.org/10.1016/j.isci.2021.102502.

ACKNOWLEDGMENTS

This work was supported by the National Key R&D Project from Minister of Science and Technology (2016YFA0202704), the National Natural Science Foundation of China (Grant No. 51775049), Beijing Natural Science Foundation (4192069), the Beijing Municipal Science and Technology Commission (Z171100000317001), Young Top-Notch Talents Program of Beijing Excellent Talents Funding (2017000021223ZK03), and Beijing Nova program (Z201100006820063).

AUTHOR CONTRIBUTIONS

Conceptualization, X.Y.C and F.W.; methodology, F.W., J.W.T., Y.X.S., X.L.T., X.L.W., and Y.F.D.; writing – original draft, F.W. and X.Y.C.; writing – review & editing, X.Y.C., Y.Y., and Z.L.W.; funding acquisition, X.Y.C. and Z.L.W.; supervision, X.Y.C., Y.Y., and Z.L.W. All the authors discussed the results and commented on the manuscript.

DECLARATION OF INTERESTS

There is no conflict of interest to declare.

Received: February 6, 2021
Revised: April 6, 2021
Accepted: April 28, 2021
Published: May 21, 2021

REFERENCES

Cheng, X., Miao, L., Song, Y., Su, Z., Chen, H., Chen, X., Zhang, J., and Zhang, H. (2017). High efficiency power management and charge boosting strategy for a triboelectric nanogenerator. Nano Energy *38*, 438–446.

Cheng, X., Tang, W., Song, Y., Chen, H., Zhang, H., and Wang, Z.L. (2019). Power management and effective energy storage of pulsed output from triboelectric nanogenerator. Nano Energy *61*, 517–532.

Fan, F.-R., Tian, Z.-Q., and Lin Wang, Z. (2012). Flexible triboelectric generator. Nano Energy *1*, 328–334.

García Núñez, C., Manjakkal, L., and Dahiya, R. (2019). Energy autonomous electronic skin. Npj Flex Electron. *3*, 1.

Harmon, W., Bamgboje, D., Guo, H., Hu, T., and Wang, Z.L. (2020). Self-driven power management system for triboelectric nanogenerators. Nano Energy *71*, 104642.

Kim, H., Rao, S.R., Kapustin, E.A., Zhao, L., Yang, S., Yaghi, O.M., and Wang, E.N. (2018). Adsorption-based atmospheric water harvesting device for arid climates. Nat. Commun. *9*, 1191.

Li, S., Fan, Y., Chen, H., Nie, J., Liang, Y., Tao, X., Zhang, J., Chen, X., Fu, E., and Wang, Z.L. (2020a). Manipulating the triboelectric surface charge density of polymers by low-energy helium ion irradiation/implantation. Environ. Sci. *13*, 896–907.

Li, S., Nie, J., Shi, Y., Tao, X., Wang, F., Tian, J., Lin, S., Chen, X., and Wang, Z.L. (2020b). Contributions of different functional groups to contact electrification of polymers. Adv. Mater. *32*, 2001307.

Liang, Y., Dong, H., Aurbach, D., and Yao, Y. (2020a). Current status and future directions of multivalent metal-ion batteries. Nat. Energy *5*, 646–656.

Liang, X., Jiang, T., Liu, G., Feng, Y., Zhang, C., and Wang, Z.L. (2020b). Spherical triboelectric nanogenerator integrated with power management module for harvesting multidirectional water wave energy. Energy Environ. Sci. *13*, 277–285.

Liang, X., Jiang, T., Feng, Y., Lu, P., An, J., and Wang, Z.L. (2020c). Triboelectric nanogenerator network integrated with charge excitation circuit for effective water wave energy harvesting. Adv. Energy Mater. *10*, 2002123.

Liu, Z., Ma, Y., Ouyang, H., Shi, B., Li, N., Jiang, D., Xie, F., Qu, D., Zou, Y., Huang, Y., et al. (2019a). Transcatheter self-powered ultrasensitive endocardial pressure sensor. Adv. Funct. Mater. *29*, 1807560.

Liu, W., Wang, Z., Wang, G., Liu, G., Chen, J., Pu, X., Xi, Y., Wang, X., Guo, H., Hu, C., and Wang, Z.L. (2019b). Integrated charge excitation triboelectric nanogenerator. Nat. Commun. *10*, 1426.

Liu, X., Gao, H., Ward, J.E., Liu, X., Yin, B., Fu, T., Chen, J., Lovley, D.R., and Yao, J. (2020a). Power generation from ambient humidity using protein nanowires. Nature *578*, 550–554.

Liu, W., Wang, Z., Wang, G., Zeng, Q., He, W., Liu, L., Wang, X., Xi, Y., Guo, H., Hu, C., and Wang, Z.L. (2020b). Switched-capacitor-convertors based on fractal design for output power management of triboelectric nanogenerator. Nat. Commun. *11*, 1883.

Mao, Y., Zhang, N., Tang, Y., Wang, M., Chao, M., and Liang, E. (2017). A paper triboelectric nanogenerator for self-powered electronic systems. Nanoscale *9*, 14499–14505.

Miao, L., Wan, J., Song, Y., Guo, H., Chen, H., Cheng, X., and Zhang, H. (2019). Skin-inspired humidity and pressure sensor with a wrinkle-on-sponge structure. ACS Appl. Mater. Interfaces *11*, 39219–39227.

Niu, S., Wang, X., Yi, F., Zhou, Y.S., and Wang, Z.L. (2015). A universal self-charging system driven by random biomechanical energy for sustainable

operation of mobile electronics. Nat. Commun. *6*, 8975.

Nyholm, L. (2020). Lighter and safer. Nat. Energy *5*, 739–740.

Ouyang, H., Liu, Z., Li, N., Shi, B., Zou, Y., Xie, F., Ma, Y., Li, Zhe, Li, H., Zheng, Q., et al. (2019). Symbiotic cardiac pacemaker. Nat. Commun. *10*, 1821.

Pu, X., Liu, M., Li, L., Zhang, C., Pang, Y., Jiang, C., Shao, L., Hu, W., and Wang, Z.L. (2016). Efficient charging of Li-ion batteries with pulsed output current of triboelectric nanogenerators. Adv. Sci. *3*, 1500255.

Ren, Z., Ding, Y., Nie, J., Wang, F., Xu, L., Lin, S., Chen, X., and Wang, Z.L. (2019). Environmental energy harvesting adapting to different weather conditions and self-powered vapor sensor based on humidity-responsive triboelectric nanogenerators. ACS Appl. Mater. Interfaces *11*, 6143–6153.

Ren, Z., Zheng, Q., Wang, H., Guo, H., Miao, L., Wan, J., Xu, C., Cheng, S., and Zhang, H. (2020a). Wearable and self-cleaning hybrid energy harvesting system based on micro/nanostructured haze film. Nano Energy *67*, 104243.

Ren, Z., Wang, Z., Liu, Z., Wang, L., Guo, H., Li, L., Li, S., Chen, X., Tang, W., and Wang, Z.L. (2020b). Energy harvesting from breeze wind (0.7–6 m s^{-1}) using ultra-stretchable triboelectric nanogenerator. Adv. Energy Mater. *10*, 2001770.

Say, M.G., Brooke, R., Edberg, J., Grimoldi, A., Belaineh, D., Engquist, I., and Berggren, M. (2020). Spray-coated paper supercapacitors. NPJ Flex Electron. *4*, 14.

Seol, M.-L., Han, J.-W., Jeon, S.-B., Meyyappan, M., and Choi, Y.-K. (2015). Floating oscillator-embedded triboelectric generator for versatile mechanical energy harvesting. Sci. Rep. *5*, 16409.

Song, Y., Wang, H., Cheng, X., Li, G., Chen, X., Chen, H., Miao, L., Zhang, X., and Zhang, H. (2019). High-efficiency self-charging smart bracelet for portable electronics. Nano Energy *55*, 29–36.

Tang, Y., Zhou, H., Sun, X., Diao, N., Wang, J., Zhang, B., Qin, C., Liang, E., and Mao, Y. (2020). Triboelectric touch-free Screen sensor for noncontact gesture recognizing. Adv. Funct. Mater. *30*, 1907893.

Tarancón, A. (2019). Powering the IoT revolution with heat. Nat. Electron. *2*, 270–271.

Wang, Z.L. (2018). Nanogenerators, self-powered systems, blue energy, piezotronics and piezo-phototronics – a recall on the original thoughts for coining these fields. Nano Energy *54*, 477–483.

Wang, M., Zhang, J., Tang, Y., Li, J., Zhang, B., Liang, E., Mao, Y., and Wang, X. (2018). Air-flow-driven triboelectric nanogenerators for self-powered real-time respiratory monitoring. ACS Nano *12*, 6156–6162.

Wang, H., Wang, J., Xia, X., Guan, D., and Zi, Y. (2020a). Multifunctional self-powered switch toward delay-characteristic sensors. ACS Appl. Mater. Interfaces *12*, 22873–22880.

Wang, H., Xu, L., Bai, Y., and Wang, Z.L. (2020b). Pumping up the charge density of a triboelectric nanogenerator by charge-shuttling. Nat. Commun. *11*, 4203.

Wang, Y., Yang, E., Chen, T., Wang, J., Hu, Z., Mi, J., Pan, X., and Xu, M. (2020c). A novel humidity resisting and wind direction adapting flag-type triboelectric nanogenerator for wind energy harvesting and speed sensing. Nano Energy *78*, 105279.

Xia, X., Fu, J., and Zi, Y. (2019). A universal standardized method for output capability assessment of nanogenerators. Nat. Commun. *10*, 4428.

Xia, X., Wang, H., Basset, P., Zhu, Y., and Zi, Y. (2020). Inductor-Free output multiplier for power promotion and management of triboelectric nanogenerators toward self-powered systems. ACS Appl. Mater. Interfaces *12*, 5892–5900.

Xu, L., Wu, H., Yao, G., Chen, L., Yang, X., Chen, B., Huang, X., Zhong, W., Chen, X., Yin, Z., and Wang, Z.L. (2018). Giant voltage enhancement *via* triboelectric charge supplement channel for self-powered electroadhesion. ACS Nano *12*, 10262–10271.

Xu, L., Xu, L., Luo, J., Yan, Y., Jia, B., Yang, X., Gao, Y., and Wang, Z.L. (2020). Hybrid all-in-one power source based on high-performance spherical triboelectric nanogenerators for harvesting environmental energy. Adv. Energy Mater. *10*, 2001669.

Xue, G., Xu, Y., Ding, T., Li, J., Yin, J., Fei, W., Cao, Y., Yu, J., Yuan, L., Gong, L., et al. (2017). Water-evaporation-induced electricity with nanostructured carbon materials. Nat. Nanotech. *12*, 317–321.

Zhang, L., Zhang, B., Chen, J., Jin, L., Deng, W., Tang, J., Zhang, H., Pan, H., Zhu, M., Yang, W., and Wang, Z.L. (2016). Lawn structured triboelectric nanogenerators for scavenging sweeping wind energy on rooftops. Adv. Mater. *28*, 1650–1656.

Zhang, Z., Li, X., Yin, J., Xu, Y., Fei, W., Xue, M., Wang, Q., Zhou, J., and Guo, W. (2018). Emerging hydrovoltaic technology. Nat. Nanotech. *13*, 1109–1119.

Zhang, B., Tang, Y., Dai, R., Wang, H., Sun, X., Qin, C., Pan, Z., Liang, E., and Mao, Y. (2019). Breath-based human–machine interaction system using triboelectric nanogenerator. Nano Energy *64*, 103953.

Zhang, N., Qin, C., Feng, T., Li, J., Yang, Z., Sun, X., Liang, E., Mao, Y., and Wang, X. (2020). Non-contact cylindrical rotating triboelectric nanogenerator for harvesting kinetic energy from hydraulics. Nano Res. *13*, 1903–1907.

Zhao, J., and You, Z. (2014). A Shoe-embedded piezoelectric energy harvester for wearable sensors. Sensors *14*, 12497–12510.

Zheng, H., Zi, Y., He, X., Guo, H., Lai, Y.-C., Wang, J., Zhang, S.L., Wu, C., Cheng, G., and Wang, Z.L. (2018). Concurrent harvesting of ambient energy by hybrid nanogenerators for wearable self-powered systems and active remote sensing. ACS Appl. Mater. Interfaces *10*, 14708–14715.

Zi, Y., Wang, J., Wang, S., Li, S., Wen, Z., Guo, H., and Wang, Z.L. (2016a). Effective energy storage from a triboelectric nanogenerator. Nat. Commun. *7*, 10987.

Zi, Y., Guo, H., Wen, Z., Yeh, M.-H., Hu, C., and Wang, Z.L. (2016b). Harvesting low-frequency (<5 Hz) irregular mechanical energy: a possible killer application of triboelectric nanogenerator. ACS Nano *10*, 4797–4805.

Zi, Y., Guo, H., Wang, J., Wen, Z., Li, S., Hu, C., and Wang, Z.L. (2017). An inductor-free auto-power-management design built-in triboelectric nanogenerators. Nano Energy *31*, 302–310.

Zuo, Z., Liu, L., Zhang, L., and Fang, Y. (2018). Indoor positioning based on Bluetooth low-energy beacons adopting graph optimization. Sensors *18*, 3736.

STAR★METHODS

RESOURCE AVAILABILITY

Lead contact

Further information and requests for resources should be directly to and will be fulfilled by the Lead Contact, Xiangyu Chen, chenxiangyu@binn.cas.cn.

Materials availability

This study did not generate new unique reagents.

Data and code availability

We do not have any code and upon request we can provide the original data.

METHOD DETAILS

Fabrication of the hard and soft universal managing circuit

The fabrication of the hard and soft universal managing circuits is respectively based on the mature printed circuit board (PCB) technology and flexible printed circuit (FPC) technology. Thus, schematic illustrations of the circuit's multilayer structures are necessary previous to the automatic production. An electronic structural design software named of Altium Designer 18 was used to depict the structural sketches which are available in Figure S15 (Supporting Information).

Fabrication of the polymer nanostructures on the surface of the PTFE thin film and materials characterization

A 50-μm-thick FEP thin film (American Durafilm) was cleaned with menthol and deionized water consecutively, blown dry with nitrogen gas and then surface sprayed gold for 20s. Then the PTFE film was dry-etched to create the nanostructures by applying the inductively coupled plasma (ICP) method: the etching time was 180 s; and the flow rate of Ar, O_2, and CF_4 gases were 25.0 sccm, 10.0 sccm, and 35.0 sccm, respectively. Field-emission scanning electron microscopy (Hitachi SU8020) was applied to investigate the surface morphology of induced nanostructures on the surface of the PTFE film.

Electric measurements device

The voltage, current, transferred charges and capacitor voltage were measured by an electrometer (Keithley 6514). The high current above 25 mA was measured by Keithley DAQ6510. The layered TENG was mounted on the programmed linear motor which was used to simulate walking action.